

Duskside auroral undulations observed by IMAGE and their possible association with large-scale structures on the inner edge of the electron plasma sheet

W. S. Lewis,¹ J. L. Burch,¹ J. Goldstein,¹ W. Horton,² J. C. Perez,² H. U. Frey,³ and P. C. Anderson⁴

Received 13 August 2005; revised 1 November 2005; accepted 9 November 2005; published 20 December 2005.

[1] On February 6, 2002 large-scale undulations along the equatorward edge of the afternoon/dusk auroral oval were observed with the IMAGE FUV/Wideband Imaging Camera (WIC) during the late expansion/recovery phase of a substorm. The undulations are similar to others previously reported, but occur at higher than usual latitudes and map to the outer duskside magnetosphere, 1 to 2 R_E beyond a plasmaspheric drainage plume. The mapping suggests that the undulations result from large-scale fluctuations on the inner edge of the electron plasma sheet. 2.5-D simulations using representative plasma parameters for this region indicate that such large-scale coherent structures can be created by a kinetic drift wave driven by the ion pressure gradient in the destabilizing curvature and grad B drift of the plasma sheet ions. **Citation:** Lewis, W. S., J. L. Burch, J. Goldstein, W. Horton, J. C. Perez, H. U. Frey, and P. C. Anderson (2005), Duskside auroral undulations observed by IMAGE and their possible association with large-scale structures on the inner edge of the electron plasma sheet, *Geophys. Res. Lett.*, 32, L24103, doi:10.1029/2005GL024390.

1. Introduction

[2] Large-scale undulations along the equatorward edge of the diffuse aurora are occasionally seen in the afternoon-evening sector during magnetically disturbed periods. First identified by *Lui et al.* [1982] in DMSP images, they have been observed from other spacecraft [*Murphree and Johnson*, 1996; *Zhang et al.*, 2005] as well and also with ground-based instruments [*Nishitani et al.*, 1994; *Baishev et al.*, 1997]. The undulations typically have wavelengths of hundreds of kilometers and amplitudes of tens to hundreds of kilometers [e.g., *Lui et al.*, 1982] and propagate westward with velocities of several hundred meters to $\sim 1 \text{ km s}^{-1}$ [e.g., *Nishitani et al.*, 1994]. Most of the reported cases have been observed at magnetic latitudes (MLAT) below 65° and often near 60° . However, *Baishev et al.* [1997] and *Zhang et al.* [2005] report examples of undulations at somewhat

higher latitudes and suggest that these result from a process different from the subauroral processes to which the lower-latitude undulations have been attributed.

[3] Processes proposed to explain the undulations include 1) a Kelvin-Helmholtz instability (KHI) in the enhanced plasma flow associated with subauroral ion drifts (SAID) [e.g., *Kelley*, 1986; *Yamamoto et al.*, 1991]; 2) a KHI in a current sheet at the equatorward edge of the diffuse proton aurora [*Yamamoto et al.*, 1993, 1994]; 3) a KHI in the sheared plasma flow associated with an auroral arc [*Baishev et al.*, 1997]; and 4) drift wave instabilities on the inner edge of the plasma sheet [*Lui et al.*, 1982; *Fedorovich*, 1988].

[4] The occurrence of undulations at “subauroral” latitudes points to a source region in the inner magnetosphere, near the plasmapause, while the higher-latitude events reported by *Baishev et al.* [1997] and *Zhang et al.* [2005] require a source farther out. There are thus two questions about the origin of the undulations: 1) Which mechanism produces them? A shear-driven instability (i.e., KHI)? An instability resulting from a density and/or temperature gradient (i.e., a drift wave)? Or some hybrid instability? And 2) where and under what conditions does this mechanism operate?

2. Observations

[5] On February 6, 2002 large-scale undulations along the equatorward edge of the auroral oval in the afternoon/dusk sector (Figure 1) were observed with the IMAGE FUV Wideband Imaging Camera (WIC) [*Mende et al.*, 2000a] during the recovery phase of a moderate magnetic storm. The undulations were observed in the $14.5\text{--}18.75$ MLT sector between 65° and 71° MLAT. They were first seen in the image acquired at 0844:14 UT, ~ 12 minutes after the onset of a substorm, and were observed until 0931:14 UT, when IMAGE began its perigee pass and FUV was switched off. The wavelength and crest-to-base length of the undulations averaged $292 \pm 72 \text{ km}$ and $224 \pm 71 \text{ km}$, respectively; and the undulations propagated westward with an average speed of $0.90 \pm 0.06 \text{ km s}^{-1}$. These values are consistent with those reported in earlier studies.

[6] The undulations varied in intensity, number, and appearance during the ~ 45 minutes when they were observable; however, poor signal-to-noise in some images renders any pattern that may underlie this variability difficult to determine. Nonetheless, it is evident that, as the recovery phase progressed, the undulations in the evening/late afternoon sector disappeared, while those at earlier local times continued to propagate westward as a coherent structure (Figures 1a and 1b). Throughout the event both

¹Space Science and Engineering Division, Southwest Research Institute, San Antonio, Texas, USA.

²Institute for Fusion Studies, University of Texas at Austin, Austin, Texas, USA.

³Space Sciences Laboratory, University of California, Berkeley, California, USA.

⁴Center for Space Sciences, University of Texas at Dallas, Richardson, Texas, USA.

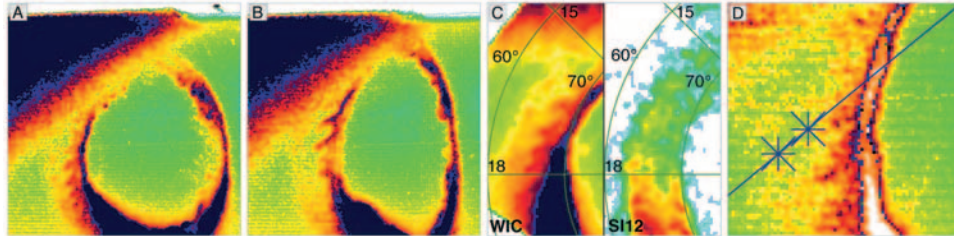


Figure 1. WIC images showing the evolution of the undulations from (a) 0900:36 UT to (b) 0918:59 UT. (c) Comparison of the WIC and SI12 images (in MLT/MLAT projection), showing the occurrence of the undulations within a broad band of proton precipitation and poleward of the equatorward edge of the proton precipitation region. (d) the DMSP F13 track overplotted on the WIC image from 0856:30 UT (stars indicate F13's position at the time the image was taken and 45 seconds later, when the spacecraft encounters the diffuse electron aurora).

the wavelength and the amplitude of the undulations were observed to increase toward earlier local times, as in the cases reported by *Lui et al.* [1982].

[7] Although readily distinguishable in the WIC images, the undulations cannot be distinguished from background in images of the proton aurora acquired with the Spectrographic Imager 12 (SI12) [Mende et al., 2000b]. Comparison of the WIC and SI12 images shows that the undulations occur within a broad (8° – 10° wide) region of proton precipitation whose equatorward boundary is located at $\sim 61.5^{\circ}$ MLAT at dusk and at $\sim 64.5^{\circ}$ MLAT at 15 MLT (Figure 1c). The crests are located several degrees poleward of the equatorward edge of the proton aurora. We note that this separation in latitude between the equatorward edge of the proton aurora and the undulations appears to be inconsistent with the assumption of *Yamamoto et al.* [1993, 1994] that the undulations result from the modulation of the equatorward edge of the proton aurora.

[8] WIC detects Lyman-Birge-Hopfield (LBH) band emissions from N_2 , which are excited primarily by electron precipitation but to which protons also contribute and which they may sometimes even dominate [Hubert et al., 2001]. Which particles are primarily responsible for the undulations reported here? DMSP F13 skimmed along the edge of one of the undulations during a pass over the afternoon-sector oval between 0856 UT and 0900 UT (Figure 1d). Particle data from this pass (Figure 2) show a region of precipitating 0.3–10 keV electrons and <10 keV protons within a broader band of 10–30 keV proton precipitation and generally coincident in MLT and MLAT with the undulation seen below the spacecraft track in the WIC image from 0856:30 UT. Comparison of the integral energy flux for the electrons and the protons (Figure 2, top) indicates that the energetic electrons play a significant—and within the energy range of the SSJ4 detector, dominant—role in exciting the diffuse emissions associated with the undulation. While the possibility of a dominant contribution from energetic protons beyond the range of the detector (i.e., >30 keV) cannot be excluded, a substantial flux of >30 keV protons would produce a noticeable signal in the SI-12, which is not seen in these data. (In this respect the February 6 event differs from those reported by *Zhang et al.* [2005], which appear to be due largely to proton precipitation.)

[9] F13 ion drift meter data (Figure 2) show that the undulations occurred in a region of sunward flow, at the poleward edge of a broad subauroral polarization stream (SAPS) [Foster and Burke, 2002]. The average flow veloc-

ity over the 65° – 71° MLAT range was $0.71 \pm 0.09 \text{ km s}^{-1}$. This value and flow direction are consistent with the velocity of the undulations estimated from the WIC images.

[10] As noted above, the undulations occurred shortly after the onset of a substorm (AE ~ 750 nT). They appeared initially in conjunction with the substorm surge [cf. *Lui et al.*, 1982] and an associated intensification that propagated rapidly westward along the main oval, and they continued to be observed after the intensification faded, well into the substorm recovery phase. The substorm was one of several that occurred during a moderate ($Dst_{min} = -82$ nT) magnetic storm that began the preceding day and was now in the recovery phase. K_p during the interval when the undulations were observed was 5-/4-, indicating moderately enhanced but weakening convection. Like the high-latitude case reported by *Zhang et al.* [2005], the undulations occurred when the magnetosphere was immersed in a high-speed ($\sim 625 \text{ km/s}$) solar wind stream, but with much lower solar wind ram pressure ($\sim 3.5 \text{ nPa}$ vs. $\sim 14 \text{ nPa}$).

3. Discussion

[11] To determine the source region of the particles responsible for the undulations, we used the Tsyganenko

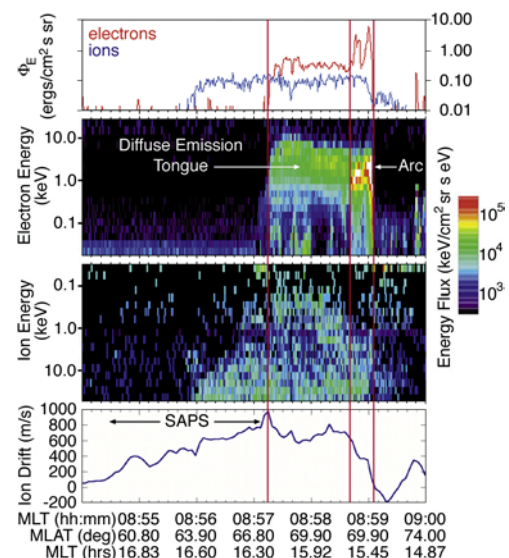


Figure 2. F13 particle and drift meter data acquired during the overflight of an emission tongue.

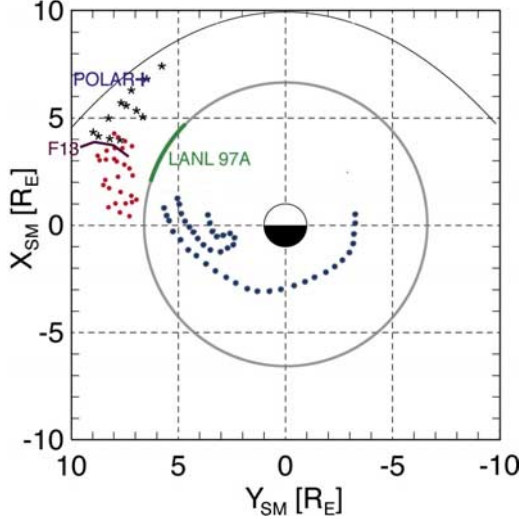


Figure 3. Auroral undulations at 0900 UT (red dots) and at 0918 UT (black stars) and the track of F13 as it crossed the oval are mapped onto the equatorial plane. The plasmapause and drainage plume locations as determined from IMAGE EUV imaging are shown, as is the approximate location of LANL 97A between 0815 UT and 1000 UT, when it encountered plume material. A decrease in spacecraft potential measured by Polar starting at \sim 0930 UT as it crossed the equatorial plane at \sim 15 MLT indicated the presence of cold plasma and the extension of the drainage plume to near the magnetopause.

2001 magnetic field model and a modified field-line tracing routine to map the undulations onto the SM X-Y plane. The mapping was performed for two different times, 0900:36 UT and 0918:59 UT, reflecting the undulations' evolution in morphology and location (cf. Figures 1a and 1b). The mapping locates the source region in the dusk/afternoon sector plasma sheet, at radial distances between \sim 7.2 R_E (crests) and \sim 9.7 R_E (troughs) and 1 to 2 R_E outside a plasmaspheric drainage plume whose presence is indicated both through images acquired with IMAGE's Extreme Ultraviolet (EUV) imager [Sandel et al., 2000] and through in-situ data acquired at geosynchronous orbit by the LANL 97A spacecraft and near the afternoon magnetopause by Polar (Figure 3). (Polar and LANL 97A data are not shown.)

[12] Like those reported by Baishev et al. [1997] and Zhang et al. [2005], the undulations described here occurred at higher than usual latitudes. Undulations at "auroral" as opposed to "subauroral" latitudes, Baishev et al. note, are not likely to be caused by a shear-driven instability in a SAID-enhanced plasma flow. As pointed out above, the auroral undulations are located in a region of westward auroral convection flow, bordering the poleward edge of a broad SAPS (Figure 2). There is no feature in the SAPS seen in the F13 data, however, that might indicate the presence of a sharp shear between the SAPS flow channel in the magnetosphere and the inner edge of the plasma sheet. Drift meter data from DMSP F15 (not shown), which crosses the oval a few minutes after F13 at a later MLT, show a stronger SAPS (peak speed = 1.2 km s^{-1}) between 58° and 61° MLAT at \sim 19.5 MLT. At this time, this portion of the oval lies just outside WIC's field of view. Images from other UTs do indicate the presence of undulations at

later MLTs, but these features are not continuously present and are often difficult to distinguish. Thus it is not possible to assess what role, if any, the SAPS observed by F15 may have played in generating the undulations.

[13] As an alternative to the shear-driven instability, a drift wave on the inner edge of the plasma sheet has been proposed to explain the auroral undulations [Lui et al., 1982; Fedorovich, 1988]. To test the drift wave hypothesis, we carried out 2.5D simulations with a pseudo-spectral code using Chebyshev polynomials for basis functions. (The pseudo-spectral code is described by Horton and Ichikawa [1996].) Because no in-situ plasma or ENA data were available for the dusk/afternoon sector outer magnetosphere, we used ion pressure profiles based on AMPTE data for comparably disturbed periods [Lui et al., 1987; De Michelis et al., 1999]. The ion pressure decreases with increasing L, while the ion density (temperature) decreases (increases) radially inward from the plasma sheet into the ring current. The strength of density, temperature, and pressure gradients is measured with respect to the radius of curvature R_c of the magnetic field in the equatorial plane, which we assumed to equal $L/3$ or $3 R_E$ at $L = 9$. For our simulation we assumed ion temperatures of 5–10 keV and that $L_{Ti} \sim -L_{ni}/2 \sim R_c \sim 3 R_E$, where L_{ni} is the ion density gradient scale length and L_{Ti} the ion temperature gradient scale length. Using the formula given by Mozer [1970], which assumes a dipole field, we mapped the ionospheric electric field derived from F13 velocity measurements in the region of the auroral undulations onto the equatorial plane and then used \mathbf{B} calculated by Tsyganenko 2001 to estimate an $\mathbf{E} \times \mathbf{B}$ convective flow speed of \sim 10 km s^{-1} . This value is consistent with the azimuthal velocity measured in the afternoon sector by LANL 97A at geosynchronous orbit.

[14] Given the assumed magnetospheric conditions, the simulations produced large-scale coherent density structures whose morphology, wavelength, and amplitude are consistent with those of the auroral undulations mapped onto the equatorial plane. Like the undulations, the density structures propagate westward, from evening toward afternoon, while growing. Figure 4 shows their evolution at two different

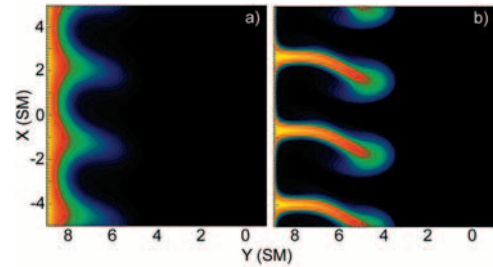


Figure 4. Images at two different simulation times showing the evolution of the ion density structures well after the saturation of the initial linear unstable growth phase. (Comparable density structures will exist for the electrons as well.) To obtain structures consistent with the morphology of the undulations observed by WIC requires a Richardson number $R_i > 100$, indicating that while the shear flow produces a slight lagging in the tips of the plasma fingers, it is not a dominant effect. False color indicates density, which ranges from 1 cm^{-3} (yellow) to 0.1 cm^{-3} (blue).

time steps in the simulation. The pronounced change in morphology, from wave-like to finger-like, during an interval of 12 to 15 minutes is similar to that observed in the auroral undulations at 0900 and 0918 UT (cf. Figure 1).

[15] The density structures in the simulation are created by a kinetic drift wave driven by the ion pressure gradient ($L_{pi}^{-1} = L_{ni}^{-1} + L_{Ti}^{-1}$) in the destabilizing magnetic curvature and $\text{grad } \mathbf{B}$ drift of the plasma sheet ions [Crabtree *et al.*, 2003]. The maximum growth rate is given by $\Gamma = \sqrt{v_{thi}^2/(R_c(1/L_{ti} - (\gamma - 1)/L_{ni}))}$, where γ is the adiabatic gas constant. The threshold for the ion drift waves is determined by this maximum growth rate minus the stabilizing contributions from (1) the square of the ion diamagnetic frequency $\omega_{*i} = k_\phi v_{di}$, where $v_{di} = T_i/eBL_{pi} + \sim 10 \text{ km s}^{-1}$ for the conditions near the center of the structures and (2) the height-integrated ionospheric Pedersen conductivity from the parallel currents driven by the convection in the magnetosphere. The conductivity contribution and ion diamagnetic drifts combine to damp the high \mathbf{k} modes, leaving only the low modes unstable when the gradients exceed the critical values. Sufficiently high cold plasma density from the plasmasphere would suppress the growth of the fingers. We did not include this effect in the simulation, however, because the undulations map well outside the plasmaspheric drainage plume.

4. Conclusion

[16] The simulation results presented here suggest that the duskside auroral undulations observed by IMAGE result from coherent, large-scale density fluctuations in the dusk/afternoon sector plasma sheet that could be driven by the drift wave instability. This finding supports the proposal by Lui *et al.* [1982] and Fedorovich [1988] regarding the possible role of drift waves in the occurrence of undulations at the equatorward edge of the diffuse aurora. We note that while low-frequency drift waves are ubiquitous in MHD-stable laboratory plasmas [Horton, 1999] and should, in principle, be relatively common in the magnetosphere as well, auroral undulations are observed only infrequently. The question thus arises, what are the global magnetospheric conditions required for these structures and the associated auroral undulations to occur? The undulations are typically observed during geomagnetic storms and in association with substorms. Thus the occurrence of the fluctuations on the plasma sheet may be correlated with storm/substorm-related changes in the central plasma sheet density or in the ion temperature in the ring current. Further work is needed to examine these possibilities as well as to identify other examples of auroral undulations that can be correlated with changes in the peaks (gradients) of the density and the ion temperature profiles as determined from contemporaneous in-situ or ENA data. Measurements from multiple satellites would be particularly useful in confirming the existence of wave structures on the inner edge of the plasma sheet.

[17] **Acknowledgments.** WSL gratefully acknowledges helpful discussions with R. A. Wolf, M. G. Henderson, G. R. Gladstone, and

M. Engebretson. The Dst, AE, and Kp indices were provided by the World Data Center in Kyoto. ACE, LANL 97A MPA, and Polar EFI data used in this study, although not shown, were obtained from the CDAWeb. We thank D. McComas (SWRI), M. Thomsen (LANL) and F. Mozer (UC Berkeley) for making these data available. This research was supported by NASA NAS5-96020 (WSL, JLB, JG, HUF), NAG5-12787 (JG) and NSF ATM 0229863 (WH and JCP).

References

- Baishev, D. G., et al. (1997), Magnetic storm-time variations of the geomagnetic field during large-scale undulations of the evening diffuse aurora, *Geomagn. Aeron.*, **37**, 706.
- Crabtree, C., W. Horton, H. V. Wong, and J. W. Van Dam (2003), Bounce-averaged stability of compressional modes in geotail flux tubes, *J. Geophys. Res.*, **108**(A2), 1084, doi:10.1029/2002JA009555.
- De Michelis, P., I. A. Daglis, and G. Consolini (1999), An average image of proton plasma pressure and of current systems in the equatorial plane derived from AMPTE/CCE-CHEM measurements, *J. Geophys. Res.*, **104**, 28,615.
- Fedorovich, G. V. (1988), The wave structure of the equatorial boundary of the zone of diffuse precipitation of auroral electrons, *Geomagn. Aeron.*, **28**, 83.
- Foster, J. C., and W. J. Burke (2002), SAPS: A new characterization for sub-auroral electric fields, *Eos Trans. AGU*, **83**, 393.
- Horton, W. (1999), Drift waves and transport, *Rev. Mod. Phys.*, **71**, 735.
- Horton, W., and Y.-H. Ichikawa (1996), *Chaos and Structures in Nonlinear Plasmas*, p. 221, World Sci., Hackensack, N. J.
- Hubert, B., J.-C. Gérard, D. V. Bisikalo, V. I. Shematovich, and S. C. Solomon (2001), The role of proton precipitation in the excitation of auroral FUV emissions, *J. Geophys. Res.*, **106**, 21,475.
- Kelley, M. C. (1986), Intense sheared flow as the origin of large-scale undulations of the edge of the diffuse aurora, *J. Geophys. Res.*, **91**, 3225.
- Lui, A. T. Y., C.-I. Meng, and S. Ismail (1982), Large amplitude undulations on the equatorward boundary of the diffuse aurora, *J. Geophys. Res.*, **87**, 2385.
- Lui, A. T. Y., R. W. McEntire, and S. M. Krimigis (1987), Evolution of the ring current during two geomagnetic storms, *J. Geophys. Res.*, **92**, 7459.
- Mende, S. B., et al. (2000a), Far ultraviolet imaging from the image spacecraft. 2. Wideband FUV imaging, *Space Sci. Rev.*, **91**, 271.
- Mende, S. B., et al. (2000b), Far ultraviolet imaging from the image spacecraft. 3. Spectral imaging of Lyman α and OI 135.6 nm, *Space Sci. Rev.*, **91**, 287.
- Mozer, F. S. (1970), Electric field mapping in the ionosphere at the equatorial plane, *Planet. Space Sci.*, **18**, 259.
- Murphree, J. S., and M. L. Johnson (1996), Clues to plasma processes based on Freja UV observations, *Adv. Space Res.*, **18**, 95.
- Nishitani, N., G. Hough, and M. W. J. Scourfield (1994), Spatial and temporal characteristics of giant undulations, *Geophys. Res. Lett.*, **21**, 2673.
- Sandel, B. R., et al. (2000), The extreme ultraviolet imager investigation for the IMAGE mission, *Space Sci. Rev.*, **91**, 197.
- Yamamoto, T., et al. (1991), A particle simulation of large-amplitude undulations on the evening diffuse auroral boundary, *J. Geophys. Res.*, **96**, 1439.
- Yamamoto, T., et al. (1993), A particle simulation of “giant” undulations on the evening diffuse auroral boundary, *J. Geophys. Res.*, **98**, 5785.
- Yamamoto, T., et al. (1994), Convective generation of “giant” undulations on the evening diffuse auroral boundary, *J. Geophys. Res.*, **99**, 19,499.
- Zhang, Y., L. J. Paxton, D. Morrison, A. T. Y. Lui, H. Kil, B. Wolven, C.-I. Meng, and A. B. Christensen (2005), Undulations on the equatorward edge of the diffuse proton aurora: TIMED/GUVI observations, *J. Geophys. Res.*, **110**, A08211, doi:10.1029/2004JA010668.

P. C. Anderson, Center for Space Sciences, University of Texas at Dallas, Richardson, TX 75083-0688, USA.

J. L. Burch, J. Goldstein, and W. S. Lewis, Space Science and Engineering Division, Southwest Research Institute, San Antonio, TX 78228-0510, USA. (wlewis@swri.edu)

H. U. Frey, Space Sciences Laboratory, University of California, Berkeley, CA 94720-7450, USA.

W. Horton and J. C. Perez, Institute for Fusion Studies, University of Texas at Austin, Austin, TX 78712-0262, USA.